Neuroimaging features of diffuse hemispheric glioma, H3 G34-mutant: a case series and systematic review

Running title: Imaging of diffuse hemispheric glioma

Ryo Kurokawa[1,*], Akira Baba[1], Mariko Kurokawa[1], Emile S Pinarbasi[2], Naohiro Makise[3], Yoshiaki Ota[1], John Kim[1], Ashok Srinivasan[1], Toshio Moritani[1]

[1]Division of Neuroradiology, Department of Radiology, University of Michigan, 1500 E. Medical Center Dr., Ann Arbor, MI, 48109, US.

[2] Department of Pathology, University of Michigan Medical School, 3510 MSRB1, 1150 W. Medical Center Dr, Ann Arbor, Michigan, 48109, US.

[3] Department of Pathology, Graduate School of Medicine, The University of Tokyo, 7-3-1 Hongo, Bunkyo-ku, Tokyo, 113-8655, Japan

* Corresponding author

Ryo Kurokawa, M.D., Ph.D.

Division of Neuroradiology, Department of Radiology, University of Michigan, Ann Arbor, Michigan

1500 E Medical Center Dr, UH B2, Ann Arbor, MI 48109.

This is the author manuscript accepted for publication and has undergone full peer review but has not been through the copyediting, typesetting, pagination and proofreading process, which may lead to differences between this version and the Version of Record. Please cite this article as doi: 10.1111/jon.12939.

Email: kuroro63@gmail.com

Phone: +1-784-219-2884

Fax: +1-734-615-9800

Keywords: diffuse hemispheric glioma, H3 G34-mutant; histone gene; systematic review; magnetic resonance imaging; computed tomography

Funding: There was no relevant funding.

Abstract

Background and Purpose

Diffuse hemispheric gliomas, H3 G34-mutant (DHGs-G34m) are newly recognized malignant brain tumors characterized by histone gene mutations. However, the neuroradiologic characteristics of these tumors require elucidation. We reviewed the demographic, clinical, and neuroradiological features of DHGs-G34m.

Methods

Data were extracted using a database search in MEDLINE, SCOPUS, and Google Scholar in June 2021. Studies assessing pathologically proven DHGs-G34m with each patient's information and neuroradiological findings were included. After screening and reviewing 332 abstracts, 12 articles including 56 cases met the criteria. We also added the findings for three patients evaluated in our hospital. Two board-certified radiologists reviewed all demographic, clinical, and neuroradiological findings of each study. One board-certified pathologist reviewed all pathological data of each study. Kaplan–Meier analyses with log-rank tests were performed to compare the survival between patients with different tumor margin characteristics (well-delineated and ill-defined).

Results

The median patient age at diagnosis was 19 years (range, 6–66 years), and 31/59 patients (52.5%) were men. Supratentorial tumors were observed in all patients (59/59, 100%). Frequent contact with leptomeninges (92.3%) and ependymal regions (87.5%) was observed. The 1- and 2-year survival rates after initial surgery were 66.7% and 40.0%, respectively.

DHGs-G34m with ill-defined and well-delineated margins showed significant differences in survival ($p = 0.04$).

Conclusions

DHGs-G34m occur most often in the supratentorial regions of adolescents. Prognosis varies among patients. Evaluation of tumor margins may provide prognostic value.

Introduction

Diffuse hemispheric gliomas, H3 G34-mutant (DHGs-G34m) are newly recognized malignant brain tumors that were identified as a result of recent advances in genetic analysis. These tumors are characterized by recurrent mutations in the histone gene H3F3A (H3.3), resulting in the substitution of glycine at position 34 with arginine or valine (G34R/V).[1,2] DHGs-G34m are most frequently located in the cerebral hemispheres, especially in the frontoparietal lobes. They commonly affect pediatric and young adult patients.

Histopathologically, DHGs-G34m present as diffusely infiltrating gliomas with astrocytic differentiation and anaplastic features, including mitotic activity, microvascular proliferation, and/or necrosis.[3] According to the Consortium to Inform Molecular and Practical Approaches to CNS Tumor Taxonomy working group in Utrecht, DHGs-G34m were suggested to be listed in the 2021 World Health Organization (WHO) classification of tumors of the central nervous system as a distinct entity from the established types of isocitrate dehydrogenase (IDH)-wildtype and IDH-mutant gliomas, including diffuse midline glioma, H3 K27M-mutant.[3] Recently published 2021 WHO classification recognized DHG-G34m as a distinct WHO grade 4 tumor.[4]

Since DHG-G34m is a recently established entity, knowledge of the neuroradiologic imaging findings of this tumor is relatively limited. To our knowledge, this study is the largest systematic review to date on the neuroradiologic features of DHGs-G34m. The purpose of this study is to summarize the demographic and clinical data of the patients and the neuroradiologic imaging features of DHGs-G34m to identify clinically relevant characteristics.

Methods

Study selection

We searched the MEDLINE via PubMed, SCOPUS, and Google Scholar databases using the following search terms on June 19th, 2021 without any language or date limits:

- ("G34") and ("neuroradiology" or "radiology" or "imaging" or "computed tomography" or "magnetic resonance" or "CT" or "MRI") for MEDLINE and Google Scholar
- ("G34") and ("neuroradiology" or "radiology" or "imaging" or "computed tomography" or "magnetic resonance" or "CT" or "MRI") within the "MEDICINE" or "NEUROSCIENCE" subcategories for SCOPUS

Publications were considered eligible if they included all of the following criteria:

1. The tumor was a pathologically proven diffuse hemispheric glioma, H3 G34-mutant with either glioblastoma-like, anaplastic astrocytoma-like, or primitive neuroectodermal tumor (PNET)-like histological features.
2. Tumor location was described.
3. Radiological findings on either CT or MRI were described, or images were provided in figures.

Exclusion criteria were as follows:

1. Missing patient-specific information and presenting with only integrated information
2. Books and conference proceedings only without a peer reviewed full-fledged publication

Additionally, the studies cited by each relevant study were also reviewed for eligibility.

We also obtained institutional review board exemption for including three unpublished cases with pathologically proven DHGs-G34m and their preoperative CT or MRI findings obtained at our hospital. Data were acquired in compliance with all applicable Health

Insurance Portability and Accountability Act regulations. This study was performed in accordance with the Preferred Reporting Items for Systematic Reviews and Meta-Analyses 2020 statement.[5]

Data analyses

Two board-certified radiologists with 9 and 13 years of experience in neuroradiology reviewed all images by consensus. We collected demographic and clinical data, including patient age and sex at diagnosis, presenting complaints, surgical procedure, chemotherapy regimen (dose, if applicable), radiation therapy (dose, if applicable), recurrence after gross total resection, the period between gross total resection and recurrence, and overall survival after the initial treatment. As for the frequency of each finding, the denominator was counted if the finding was mentioned in the manuscript or could be evaluated from figures or tables in the collected studies. When there was no description of each finding (e.g., treatment method), it was not included in the denominator or numerator.

Among radiological findings, we evaluated the following parameters:

- Tumor size, location, and margin (ill-defined or well-delineated)

- Main morphology (infiltrating, round/oval, or exophytic)
- Predominant tumor attenuation on CT
- Predominant tumor signal intensities on T2-weighted images, T1-weighted images, and fluid-attenuated inversion recovery (FLAIR) images
- Enhancement pattern on gadolinium-enhanced MRI (homogeneous, ring, patchy, nodular, heterogeneous, minimal, or none)
- Diffusion restriction and apparent diffusion coefficient value when available
- Remote lesions: considered positive if observed in the figures or mentioned in the manuscript
- Intratumoral hemorrhage: considered positive if the tumor showed high intensity on fat-suppressed T1-weighted images or hypointensity with a blooming effect on T2*-weighted images or susceptibility-weighted imaging or if this finding was mentioned in the manuscript
- Intratumoral calcification: determined on CT if it was not mentioned in the manuscript
- Cystic/necrotic change

- Dural attachment: considered positive if clearly observed in the figures or mentioned in the manuscript.
- Leptomeningeal contact: considered positive when dural or pial thickening or enhancement was present at the point of contact with the tumor on MRI or mentioned in the manuscript.
- Ependymal contact: considered positive when the tumor appeared to protrude into the ventricles on MRI or mentioned in the manuscript.
- MR spectroscopy findings (presence or absence of increased choline/ N-acetyl aspartate (NAA) ratio and lipid/lactate peak)
- Perfusion MRI findings (elevated or not)

Analysis of pathological data in the literature was performed by a board-certified pathologist with 9 years of experience in neuropathology. The pathologist evaluated the descriptions and figures related to the pathological features of each tumor in all included studies.

Statistical analyses

Log-rank tests were performed for Kaplan–Meier curve comparisons of survival in relation to the margin characteristics (well-delineated and ill-defined), necrotic/cystic changes (presence and absence), and the histologic phenotypes. Two-sided P-values < 0.05 were considered statistically significant. Statistical analyses were performed using R software (version 4.0.0; R Foundation for Statistical Computing, Vienna, Austria).

Results

Study selection

A total of 332 abstracts were screened, of which 53 potentially eligible articles were selected for further review. After excluding 41 articles and including one article extracted from the citation review of each relevant article (no case with pathologically proven DHG-G34m, 25 articles; no radiological findings or images (14 articles); insufficient patient-specific information (2 articles)), 12 articles met the selection criteria for the systematic review.[1,6-16]

The year of publication of the selected articles ranged from 2017 to 2021. With the additional three cases from our hospital, the final study cohort included 59 cases of DHG-G34m.

Demographic data

Patient demographics are summarized in Table 1. The median patient age at diagnosis was 19 years (range, 6–66 years), and 31/59 (52.5%) patients were male. The majority of patients were between 10-19 years of age (26/51 [51.0%]), followed by those aged 20-29 years (12/51 [23.5%]) and 30-39 years (7/51 [13.7%]). The ages of eight patients in one study were not included in the calculation because that study did not include information regarding the age of each patient but provided data for the number of men and women (2 men and 6 women),[8] which enabled us to determine the sex distribution for the entire population of 59 patients.

Clinical findings

Clinical data are summarized in Table 1. The most frequent presenting complaint was raised intracranial pressure symptoms including headache, nausea, vomiting, and blurred vision (19/33, 57.6%), followed by focal deficits (9/33, 27.3%) and seizures (7/33, 21.2%). Most

patients were treated with surgical resection and adjuvant chemoradiotherapy. Among chemotherapy regimens, temozolomide (12/15, 80.0%) was used most frequently. Cisplatin, vincristine, nimustine chloride, and the VCP regimen (vincristine, CCNU [lomustine], prednisone) were used in one case each (1/15, 6.7% each). Gross total resection, partial resection, and biopsy were performed in 16/37 (43.2%; including three our cases), 7/37 (18.9%), and 14/37 (37.8%), respectively. The majority of the patients (26/35, 74.3%) died, with a median overall survival period of 13.6 months (range, 0.1–55.4 months). The survival rate after initial surgery was 22/33 (66.7%) at 1 year, 12/30 (40.0%) at 2 years, and 7/28 (25.0%) at 3 years. The demographic, clinical, and histopathological characteristics of the three cases in our hospital are summarized in Table 2.

Pathological/ molecular findings

The pathological/molecular findings are summarized in Table 1. G34R and G34V mutations were observed in 47/59 (79.7%) and 3/59 (5.1%), respectively. Detailed information of mutation status was missing in the other 9/59 patients (15.3%). Histologically, the tumors showed glioblastoma (35/59, 59.3%), anaplastic astrocytoma (13/59, 22.0%), PNET-like

(8/59, 13.6%), or high-grade glioma, not otherwise specified (3/59, 5.1%) with high Ki-67 index (median, 40%) and brisk mitotic activity (18/18, 100%). Other molecular features included O[6]-methylguanine-DNA methyltransferase (MGMT) promoter-methylation (17/19, 89.5%) and glial fibrillary acidic protein immunostaining (26/27, 96.3%), while no mutation was reported related to telomerase reverse transcriptase (TERT) promoter, IDH, BRAF, or Oligodendrocyte Transcription Factor 2 (Olig2).

Radiological findings

The radiological findings are summarized in Table 3. Supratentorial tumors were observed in all the patients (59/59, 100%). Of the 38 cases where images were available for reference, 35 cases (92.1%) showed hemispheric localization. Involvement of the brainstem and cerebellum was observed in one patient (1.7%). The tumor mainly showed CT hyperdensity, T2-weighted /FLAIR hyperintensity, T1-weighted hypointensity, diffusion restriction, and various patterns of enhancement. The tumor margin was frequently ill-defined (30/47, 63.8%). Most tumors were unifocal (37/42, 88.1%) and showed leptomeningeal contact (36/39, 92.3%) and ependymal contact (21/24, 87.5%). Spinal DHG-G34m was only seen in one patient with

cerebrospinal fluid dissemination as multiple intradural extramedullary lesions.[9] Intratumoral hemorrhage and cystic/necrotic changes were observed in 19/45 (42.2%) and 28/57 (49.1%) patients, respectively. When available, a lipid/lactate peak and increased choline/NAA ratio were observed in approximately half of the patients who underwent MR spectroscopy (7/12, 58.3%). Elevated cerebral blood flow was found in 1/2 (50.0%) and 7/11 (63.6%) patients on arterial spin labeling and dynamic susceptibility contrast perfusion MRI, respectively. Figures 1–3 demonstrate the neuroradiological and pathological features of the three cases from our hospital.

Clinicoradiological correlation

Kaplan–Meier curves with a log-rank test showed a significantly unfavorable prognosis for survival in patients with tumors with an ill-defined margin (Figure 1) in comparison with those with a well-delineated margin ($p = 0.04$, Figures 2–4). No significant difference was found in survival between the histologic phenotypes, or cystic/necrotic changes (presence or absence).

Discussion

We reviewed and summarized the demographic, clinical, and radiological findings of 56 cases of diffuse hemispheric glioma, H3 G34-mutant reported in 12 publications and three additional unpublished cases. DHGs-G34m occurred most frequently in the frontal and parietal lobes in adolescent patients and young adults, and the tumors showed a high frequency of contact with the leptomeninges and ependymal region. Tumor margin characteristics were associated with the survival prognosis. To our knowledge, this is the largest systematic review of the clinicoradiological features of DHGs-G34m, which was newly listed as WHO grade 4 brain tumors in the 2021 WHO classification.[4]

Chromatin is composed of nucleosomes and their associated proteins, including an octamer composed of two copies each of the histones H3, H4, H2A, and H2B. Recurrent mutations in the histone genes H3F3A (H3.3), HISTIH3B, and HISTIH3C have been identified in a subset of high-grade gliomas, namely, diffuse midline glioma, H3 K27M-mutant, and DHG-G34m.[2,17] These mutations result in the substitution of lysine amino acid at position 27 with methionine (K27M) or glycine at position 34 with arginine or valine (G34R/V). The K27M mutation in the H3 histone gene suppresses di- and tri-methylation in H3 histones, promoting oncogenesis.[18] In contrast, the tumorigenic mechanism associated with the H3

G34-mutation remains to be determined.[1] In molecular assessments, DHGs-G34m is characterized by a lack of transcription factor Olig2 expression, as well as frequently observed features such as alpha thalassemia/mental retardation syndrome X-linked mutation, MGMT promoter methylation, BRAF V600E mutation-negative status, and isocitrate dehydrogenase-wildtype and TERT promoter-wildtype statuses.[1,15] The high frequency of a PNET-like morphology, a feature of DHGs-G34m, may be attributable to the characteristic Olig2 inactivation. This is because epigenetic Olig2 inactivation has been known to prevent neural lineage commitment in embryonic stem cells,[19,20] where DHGs-G34m is considered to arise.[20]

DHGs-G34m have been predominantly found in adolescents and young adults, with a reported median age of 14–18.0 years at diagnosis.[21-23] The median age extracted in this systematic review (19 years [range, 6–66 years]), which did not include these studies, was close to the results, and most patients were aged 10-19 years, followed by those aged 20-29 years. In their meta-analysis in 2017, Mackay et al. found that DHGs-G34m were associated with a significantly longer overall survival (median, 18.0 months; 2-year overall survival, 27.3%) than diffuse midline glioma, H3 K27M-mutant.[22] Although the overall survival in this

study (13.6 [0.1-55.4] months) was shorter than that reported in their study, the 2-year overall survival was higher (40.0%) in our study. This discrepancy indicates the variability in prognosis among patients with DHGs-G34m. This variability can be attributed to heterogeneity in the histological characteristics, including glioblastoma, anaplastic astrocytoma, and PNET-like morphology.[24]

Regarding the neuroradiological findings of DHGs-G34m, one characteristic feature found in this study was the high frequency of contact with the leptomeninges and ependymal region on preoperative MRI, which were found in 92.3% and 87.5% of the cases, respectively. This might be explained by the fact that DHGs-G34m tend to form bulky masses in the cerebral hemispheres. However, multifocal tumors were only observed in 11.9% of patients. The gap between the frequency of leptomeningeal and ependymal contact and the incidence of multifocal tumors may suggest that DHGs-G34m require time to cause CSF dissemination and subependymal tumor growth after these contacts occur. However, further studies are required to determine whether this temporal interval is unique to DHGs-G34m. A recent study identified ependymal contact in the majority of glioblastomas (237/357, 66%), and observed ventricular invasion of the tumors in only 34/237 patients (14.3%).[25] The authors also found

that tumor invasion into the ventricles was inhibited via a non-mechanical force in the ependymal region.[25]

Notably, significant differences were observed in the survival prognosis of patients with DHGs-G34m showing ill-defined margins and those with DHGs-G34m showing well-delineated margins in this study, although no significant difference was found between the histologic phenotypes. Importantly, invasion of gliomas can occur in normal-appearing surrounding parenchyma on conventional MRI.[26] However, the association between survival prognosis and tumor margin characteristics may be supported by studies on the relationships between survival prognosis and the presence and tumor proliferative activity in the neighboring brain parenchyma in patients with glioblastoma.[27,28] The nature of the tumor margin may also contribute to the diversity of prognosis in patients with DHGs-G34m in addition to histological heterogeneity, which we have described above.

This study had some limitations. First, the number of patients was small because of the rarity and novelty of this entity. Second, there were missing data and heterogeneity in the

collected studies. Missing data might have introduced bias in the frequency calculation. We calculated the frequencies of the findings from the cases where that were mentioned or that could be analogized from the figures or tables, and other cases were excluded from the calculation. Therefore, the frequency of each finding could have been higher or lower. The follow-up period (one month to several years) and the modality and sequence varied among the studies, which might have contributed to the heterogeneity of this study. Third, the imaging data were obtained by reviewing the findings of conventional MRI sequences. Data from advanced neuroradiological techniques, such as O-(2-[18F]-fluoroethyl)-L-tyrosine PET may further enhance our understanding of DHGs-G34m.[29]

In conclusion, DHGs-G34m occur most frequently in the frontal and parietal lobes in adolescent patients and young adults, and show a high frequency of hemispheric localization, resulting in contact with the leptomeninges and ependymal region. Evaluation of tumor margins may provide a prognostic value. Awareness of these characteristic neuroradiological features may provide radiologists with better recognition of this novel entity.

Acknowledgements and Disclosure

We would like to thank Editage [http://www.editage.com] for editing and reviewing this manuscript for English language.

The authors declare that they have no competing interests.

References

1. Lim KY, Won JK, Park C-K, et al. H3 G34-mutant high-grade glioma. Brain Tumor Pathol 2021;38:4-13.

2. Schwartzentruber J, Korshunov A, Liu X-Y, et al. Driver mutations in histone H3.3 and chromatin remodelling genes in paediatric glioblastoma. Nature 2012;482:226-31.

3. Louis DN, Wesseling P, Aldape K, et al. cIMPACT-NOW update 6: new entity and diagnostic principle recommendations of the cIMPACT-Utrecht meeting on future CNS tumor classification and grading. Brain Pathol 2020;30:844-56.

4. Louis DN, Perry A, Wesseling P, et al. The 2021 WHO classification of tumors of the central nervous system: a summary. Neuro Oncol 2021;23:1231-51

5. Page MJ, McKenzie JE, Bossuyt PM, et al. The PRISMA 2020 statement: an updated guideline for reporting systematic reviews. BMJ 2021;372:n71.

6. Yoshimoto K, Hatae R, Sangatsuda Y, et al. Prevalence and clinicopathological features of H3.3 G34-mutant high-grade gliomas: a retrospective study of 411 consecutive glioma cases in a single institution. Brain Tumor Pathol 2017;34:103-12.

7. Puntonet J, Dangouloff-Ros V, Saffroy R, et al. Historadiological correlations in high-grade glioma with the histone 3.3 G34R mutation. J Neuroradiol 2018;45:316-22.

8. Vettermann FJ, Felsberg J, Reifenberger G, et al. Characterization of diffuse gliomas with histone H3-G34 mutation by MRI and dynamic 18F-FET PET. Clin Nucl Med 2018;43:895-8.

9. Andreiuolo F, Lisner T, Zlocha J, et al. H3F3A-G34R mutant high grade neuroepithelial neoplasms with glial and dysplastic ganglion cell components. Acta Neuropathol Commun 2019;7:78.

10. Gonçalves FG, Alves CAPF, Vossough A. Updates in pediatric malignant gliomas. Top Magn Reson Imaging 2020;29:83-94.

11. Cheng Y, Bao W, Wu Q. Cerebral hemispheric glioblastoma with PNET-like morphology and histone H3.3 G34 mutation in younger patients: Report of three rare cases and diagnostic pitfalls. Indian J Pathol Microbiol 2020;63:262-6.

12. Onishi S, Amatya VJ, Karlowee V, et al. Radiological and immunostaining characteristics of H3.3 G34R-mutant glioma: A report of 3 cases and review of the literature. Pediatr Neurosurg 2020;55:319-25.

13. Wood MD, Neff T, Nickerson JP, et al. Post-treatment hypermutation in a recurrent diffuse glioma with H3.3 p.G34 Mutation. Neuropathol Appl Neurobiol 2021;47:460-3.

14. Kay MD, Pariury HE, Perry A, Winegar BA, Kuo PH. Extracranial metastases from glioblastoma with primitive neuronal components on FDG PET/CT. Clin Nucl Med 2020;45:e162-4.

15. Picart T, Barritault M, Poncet D, et al. Characteristics of diffuse hemispheric gliomas, H3 G34-mutant in adults. Neurooncol Adv 2021;3:vdab061.

16. Hodgson JM, Douch C, Hartley L, Merve A, Devadass A, Chatterjee F. Problem solving in clinical practice: an unusual cause of multifocal brain lesions. Arch Dis Child Educ Pract Ed 2020. [Epub ahead of print]

17. Khuong-Quang D-A, Buczkowicz P, Rakopoulos P, et al. K27M mutation in histone H3.3 defines clinically and biologically distinct subgroups of pediatric diffuse intrinsic pontine gliomas. Acta Neuropathologica 2012;124:439-47.

18. Harutyunyan AS, Krug B, Chen H, et al. H3K27M induces defective chromatin spread of PRC2-mediated repressive H3K27me2/me3 and is essential for glioma tumorigenesis. Nat Commun 2019;10:1262.

19. Sturm D, Witt H, Hovestadt V, et al. Hotspot mutations in H3F3A and IDH1 define distinct epigenetic and biological subgroups of glioblastoma. Cancer Cell 2012;22:425-37.

20. Sturm D, Bender S, Jones DTW, et al. Paediatric and adult glioblastoma: multiform (epi) genomic culprits emerge. Nat Rev Cancer 2014;14:92-107.

21. Korshunov A, Ryzhova M, Hovestadt V, et al. Integrated analysis of pediatric glioblastoma reveals a subset of biologically favorable tumors with associated molecular prognostic markers. Acta Neuropathol 2015;129:669-78.

22. Mackay A, Burford A, Carvalho D, et al. Integrated molecular meta-analysis of 1,000 pediatric high-grade and diffuse intrinsic pontine glioma. Cancer Cell 2017;32:5200-37.e5.

23. Neumann JE, Dorostkar MM, Korshunov A, et al. Distinct histomorphology in molecular subgroups of glioblastomas in young patients. J Neuropathol Exp Neurol 2016;75:408-14.

24. Korshunov A, Capper D, Reuss D, et al. Histologically distinct neuroepithelial tumors with histone 3 G34 mutation are molecularly similar and comprise a single nosologic entity. Acta Neuropathol 2016;131:137-46.

25. Li K, Song H, Wang C, et al. The ependymal region prevents glioblastoma from penetrating into the ventricle via a nonmechanical force. Front Neuroanat 2021;15:42.

26. Price SJ, Jena R, Burnet NG, et al. Improved delineation of glioma margins and regions of infiltration with the use of diffusion tensor imaging: An image-guided biopsy study. AJNR Am J Neuroradiol 2006;27:1969-74.

27. Mangiola A, de Bonis P, Maira G, et al. Invasive tumor cells and prognosis in a selected population of patients with glioblastoma multiforme. Cancer 2008;113:841-6.

28. Tejada S, Becerra-Castro MV, Nuñez-Cordoba J, Diez-Valle R. Ki-67 proliferative activity in the tumor margins as a robust prognosis factor in glioblastoma patients. J Neurol Surg A Cent Eur Neurosurg 2021;82:53-8.

29. Lohmann P, Stavrinou P, Lipke K, et al. FET PET reveals considerable spatial differences in tumour burden compared to conventional MRI in newly diagnosed glioblastoma. Eur J Nucl Med Mol Imaging 2019;46:591-602.

Tables

Table 1. Clinical and pathological characteristics of diffuse hemispheric glioma, H3 G34-mutant

Clinical	
Median age at diagnosis (years [range]) (n = 51*)	19 [6–66]
Sex	Male = 31, Female = 28
Surgical procedure	
Gross total resection	16/37 (43.2%)
Partial resection	7/37 (18.9%)
Biopsy	14/37 (37.8%)
Chemotherapy	18/20 (90.0%)
Temozolomide	12/18 (66.7%)
Others	4/18 (22.2%)
Not described	3/18 (16.7%)
Radiotherapy	19/20 (95.0%)
Dose (median [range]) (n = 9)	60 Gray [52–61.2]
Recurrence after total resection	11/16 (68.8%)

Period between initial surgery and recurrence (n = 9)	23 months [5–97]
Patient survival	9/35 (25.7%)
Follow up duration (median [range]) (n = 35)	15 months [0.1–99]
Overall survival (median [range]) (n = 26)	13.6 months [0.1–55.4]
Pathological	
G34-mutation status	
G34R	47/59 (79.7%)
G34V	3/59 (5.1%)
Not described	9/59 (15.3%)
Histology	
Glioblastoma	35/59 (59.3%)
Anaplastic astrocytoma	13/59 (22.0%)
Primitive Neuro-Ectodermic Tumor-like	8/59 (13.6%)
High-grade glioma, not otherwise specified	3/59 (5.1%)
Ki-67 (median [range]) (n = 26)	40% [7.3–95]
Brisk mitotic activity (≥15/10 high-power fields)	18/18 (100%)
p53-mutation	41/49 (83.7%)

ATRX mutation	40/46 (87.0%)
MGMT promoter-methylation	17/19 (89.5%)
TERT promoter-mutation	0/8 (0%)
IDH mutation	0/37 (0%)
BRAF mutation	0/28 (0%)
Olig2 immunostaining	0/44 (0%)
GFAP immunostaining	26/27 (96.3%)

* Eight patients in one study were excluded from the calculation because detailed age of each patient was not available.[8] n, number; ATRX, Alpha thalassemia/mental retardation syndrome X-linked; MGMT, O[6]-methylguanine-DNA methyltransferase; TERT, telomerase reverse transcriptase; IDH, isocitrate dehydrogenase; Olig2, oligodendrocyte transcription factor-2; GFAP, glial fibrillary acidic protein; G, glycine; R, arginine; V, valine.

Table 2. Clinical and pathological characteristics of the three cases of diffuse glioma, H3 G34-mutant in our hospital

	Patient 1	Patient 2	Patient 3
Clinical characteristics			
Age/sex	16/Female	22/Male	19/Female
Presenting complaint	Left facial	Bifrontal	Headache, Nausea/Vomiting,

	twitching	headache	Blurred vision
Surgical procedure	Gross total resection	Gross total resection	Gross total resection
Adjuvant chemotherapy regimen	Temozolomide + Lomustine	Temozolomide	Planned
Radiation therapy	59.4 Gy	60.0 Gy	Planned
Recurrence, the period from operation (months)	No	No	No
Current status	Alive	Alive	Alive
Follow-up duration/survival time since initial operation	16 months	10 months	1 month
Pathological			
G34 mutation status	G34R	G34R	G34R
Histology	PNET-like	Glioblastoma	Glioblastoma
Ki-67 index	>25%	>20%	>20%
Brisk mitotic activity (≥15/10 HPF)	Positive	Positive	Positive
p53 mutation	Negative	Positive	Positive
ATRX mutation	Positive	Positive	Positive

MGMT promoter-methylation	Positive	Positive	Positive
IDH status	Wild	Wild	Wild
BRAF mutation	Negative	Negative	Negative
Olig2 immunostaining	Negative	Negative	Negative
GFAP immunostaining	Positive	Positive	Positive

PNET, primitive neuroectodermal tumor; HPF, high power fields; MGMT, O[6]-methylguanine-DNA methyltransferase; ATRX, Alpha thalassemia/mental retardation syndrome X-linked; Olig2, oligodendrocyte transcription factor-2; IDH, isocitrate dehydrogenase; Gy, Gray; G, glycine; R, arginine

Table 3. Radiological characteristics of diffuse glioma, H3 G34-mutant

Parameters	
Size (mm [range]) (number = 5)	29–68
Location	
Frontal	31/59 (52.5%)
Parietal	33/59 (55.9%)
Occipital	7/59 (11.9%)
Temporal	19/59 (32.2%)
Corpus callosum	11/59 (18.6%)
Basal ganglia	8/59 (13.6%)
Brain stem	1/59 (1.7%)
Cerebellum	1/59 (1.7%)
Multifocal	5/42 (11.9%)
Morphology	
Infiltrating	25/38 (65.8%)
Round/oval	17/38 (44.7%)

Exophytic	3/38 (7.9%)
Margin	
Well-delineated	17/47 (36.2%)
Ill-defined	30/47 (63.8%)
Contrast enhancement	
Any	42/53 (79.2%)
Ring	8/53 (15.1%)
Patchy	6/53 (11.3%)
Nodular	9/53 (17.0%)
Serpiginous	5/53 (9.4%)
Minimal	17/53 (32.1%)
Predominant CT attenuation	
Hyperdense	8/9 (88.9%)
Isodense	1/9 (11.1%)
Hypodense	0
Predominant signal intensity	
T2-weighted image	

High intensity	29/35 (82.9%)
Iso intensity	5/35 (14.3%)
Low intensity	1/35 (2.9%)
T1-weighted image	
High intensity	0
Iso intensity	0
Low intensity	12/12 (100%)
Fluid-attenuated inversion recovery	
High intensity	25/25 (100%)
Iso intensity	0
Low intensity	0
Diffusion restriction	25/26 (96.2%)
Mean ADC (10^{-3} mm^2/s) [range] (number = 6)	0.694 [0.539–0.810]
MR spectroscopy: lipid/lactate peak and/or increased choline/NAA ratio*	7/12 (58.3%)
Intratumoral hemorrhage	19/45 (42.2%)
Intratumoral calcification	4/18 (22.2%)

Cystic/necrotic change	28/57 (49.1%)
Leptomeningeal contact	36/39 (92.3%)
Dural attachment	11/39 (28.2%)
Ependymal contact	21/24 (87.5%)
Cerebral blood flow on ASL	
Elevated	1/2 (50.0%)
Decreased	1/2 (50.0%)
Cerebral blood flow on contrast perfusion MRI	
Elevated	7/11 (63.6%)
Not elevated**	4/11 (36.4%)

ADC, apparent diffusion coefficient; NAA, N-acetyl aspartate; ASL, arterial spin labeling

*Both lipid/lactate peak and increased choline/NAA ratio were observed in 4 cases; at least one of these findings was observed in other 3/9 cases.[14]

**No mention of whether there was a decrease or not.[14]

Figure legends

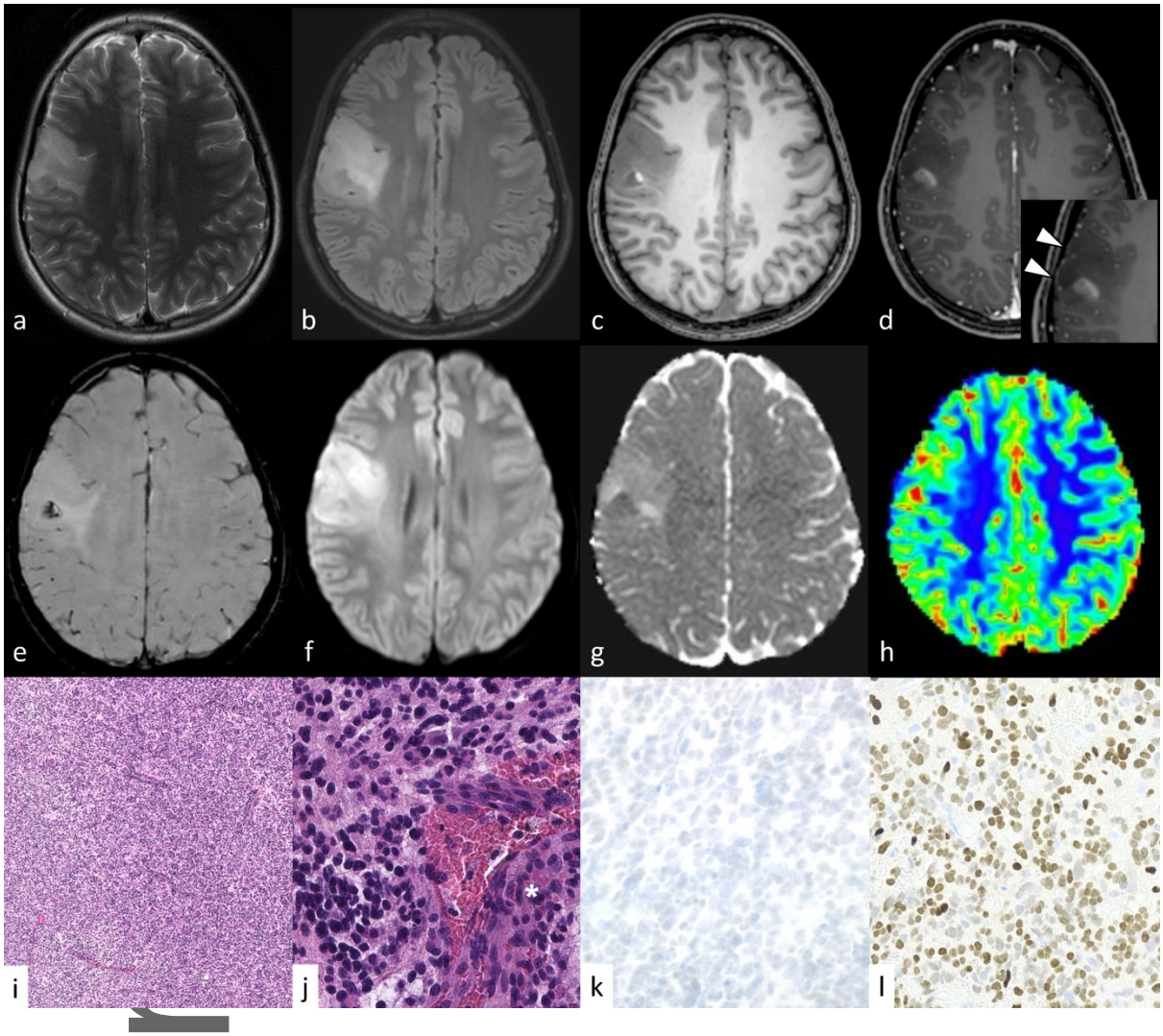

Figure 1. Diffuse hemispheric glioma, H3 G34R-mutant in a 16-year-old female presenting with left face twitching (case 1). MRI shows a 4.0 × 3.7 × 3.6 cm tumor with leptomeningeal contact laterally (d, arrowheads in the magnified view) and an ill-defined margin medially in the right frontal lobe. The tumor shows hyperintensity on T2-weighted image (a) and a fluid-attenuated inversion recovery image (b) and hypointensity on T1-weighted image (c).

Patchy enhancement was observed on fat-suppressed contrast-enhanced T1-weighted image (d). T2*-weighted image shows a hypointensity area indicating intratumoral hemorrhage (e). The tumor shows diffusion restriction with a mean apparent diffusion coefficient value of the enhancing area of 0.800×10^{-3} mm^2/s (f, g). The enhancing area shows an elevated cerebral blood flow on dynamic susceptibility contrast perfusion MRI (h). Hematoxylin and eosin stain images at low power (i, 4x) and high power (j, 40x) show a densely cellular, infiltrative tumor composed of cells with minimal cytoplasm and rounded, hyperchromatic nuclei, multinucleation and brisk mitotic activity. Microvascular proliferation is observed (j, *). Necrosis is not present. Immunohistochemical stain is negative for oligodendrocyte transcription factor-2 (k) and positive for H3 G34R (l). While the morphology is evocative of a primitive neuroectodermal tumor, the immunohistochemical profile is diagnostic of diffuse hemispheric glioma, H3 G34R-mutant.

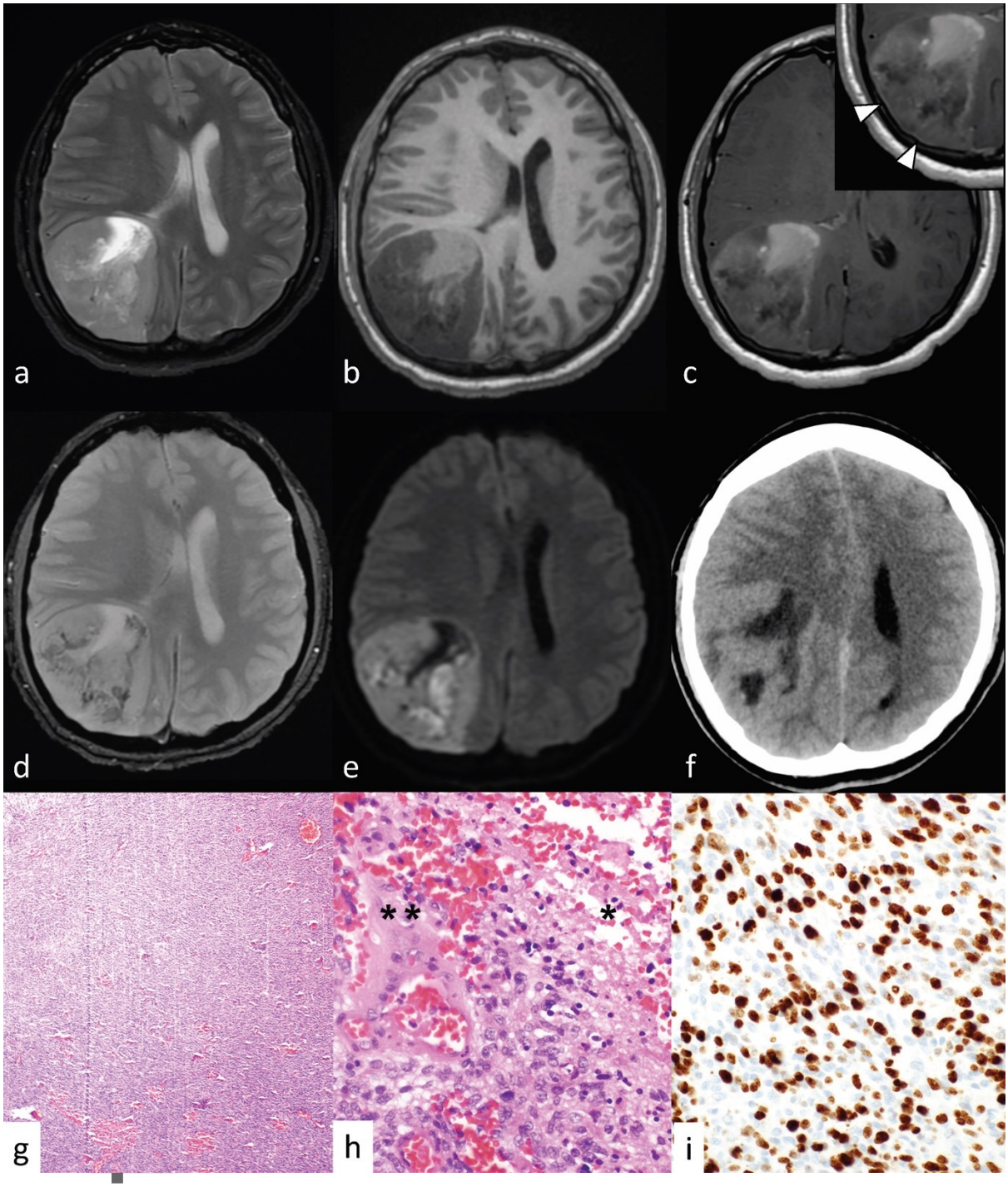

Figure 2. Diffuse hemispheric glioma, H3 G34R-mutant in a 22-year-old male presenting with an ongoing bifrontal headache for one month (case 2). MRI shows a 6.4 × 6.0 × 6.3 cm

(anteroposterior × transverse × craniocaudal) well-delineated tumor with dural attachment in the right parietal lobe (c, arrowheads in the magnified view). Axial fat-suppressed T2-weighted image show high intensity with necrosis (a). Axial T1-weighted image shows hypointensity (b) and fat-suppressed contrast-enhanced T1-weighted image shows heterogeneous enhancement (c). T2*-weighted image shows intratumoral hemorrhage (d). The tumor shows diffusion restriction with a mean apparent diffusion coefficient value of 0.599×10^{-3} mm^2/s for the enhancing area (e). The solid portion of the tumor appears hyperdense on non-enhanced axial CT without calcification (f). Hematoxylin and eosin stain images at low power (g, 4x) and high power (h, 40x) show a highly cellular infiltrative glial tumor composed of cells with high nuclear-to-cytoplasmic ratio with a focal fascicular growth pattern, palisading necrosis (h, *) and microvascular proliferation (h, **). Immunohistochemical stain for Ki-67 shows a proliferation index of greater than 20% (i). Tumor cells are negative for and oligodendrocyte transcription factor-2 and positive for H3 G34R (not shown). This case demonstrates the morphologic immunohistochemical features typical of glioblastoma.

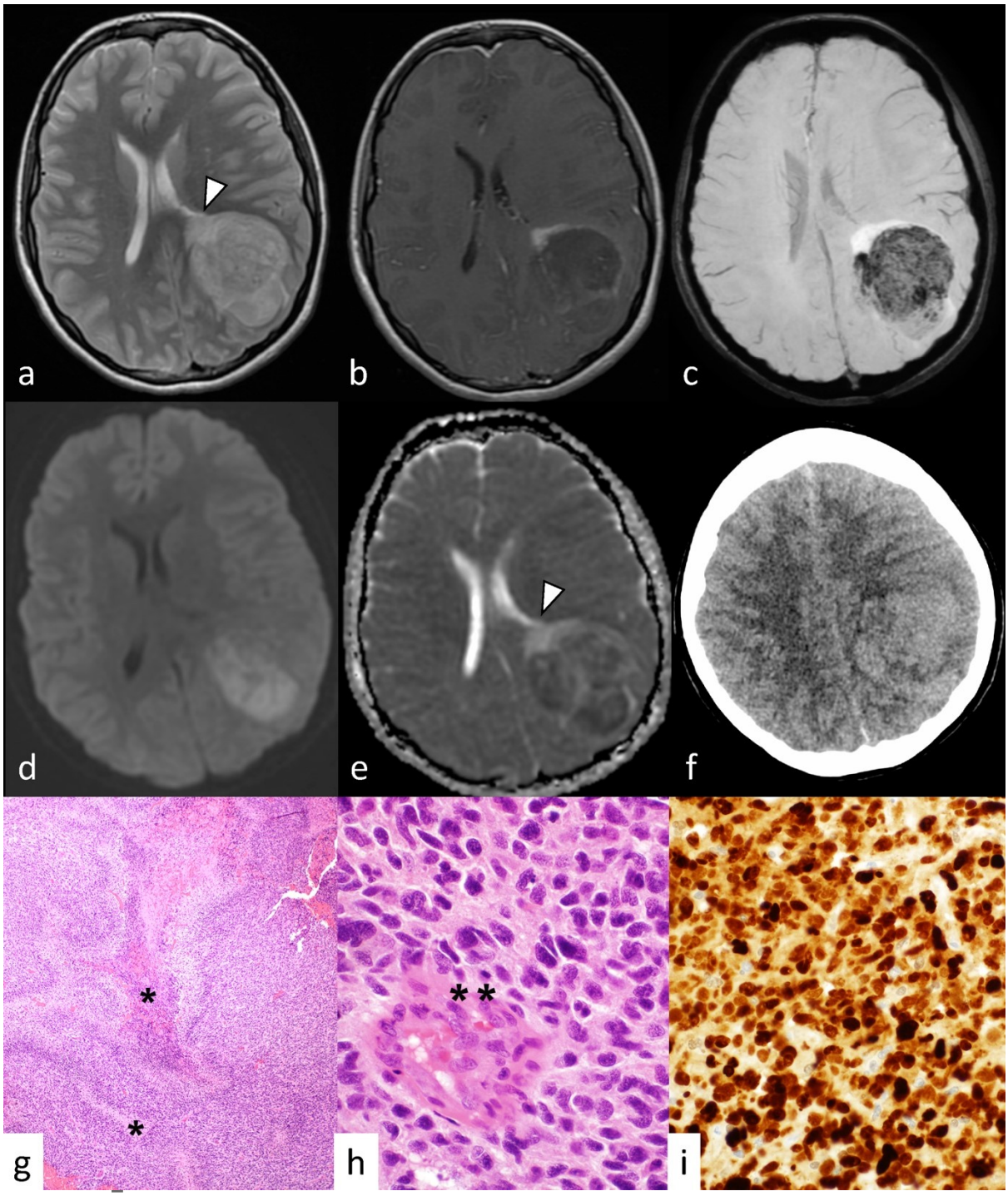

Figure 3. Diffuse hemispheric glioma, H3 G34R-mutant in a 19-year-old female presenting with headache, nausea/vomiting, and blurred vision (case 3). MRI shows a 6.0 × 5.4 × 5.1 cm

(anteroposterior × transverse × craniocaudal) well-delineated tumor with ependymal contact in the left parietal lobe (arrowheads). The tumor shows hyperintensity on T2-weighted image (a) and hypointensity on T1-weighted image (not shown) with a patchy enhancement anteriorly on fat-suppressed contrast-enhanced T1-weighted image (b). T2*-weighted image shows hypointensity indicating intratumoral hemorrhage (c). The tumor shows diffusion restriction with a mean apparent diffusion coefficient value of 0.539×10^{-3} mm^2/s for the enhancing area (d, e). The tumor shows hyperdensity on CT without calcification (f). Hematoxylin and eosin stain images at low power (g, 4x) and high power (h, 40x) show an infiltrative glial tumor with dense cellularity, brisk mitoses, necrosis (g, *), and vascular endothelial proliferation (h, **). Immunohistochemical stains demonstrate that tumor cells are positive for glial fibrillary acidic protein (not shown) and negative for oligodendrocyte transcription factor-2 (not shown) and are positive for H3 G34R (i). Ki67 shows a proliferation index >20% (not shown). These features are all characteristic of glioblastoma. Together with the H3 G34R mutation, this is diagnostic of diffuse hemispheric glioma, H3 G34-mutant.

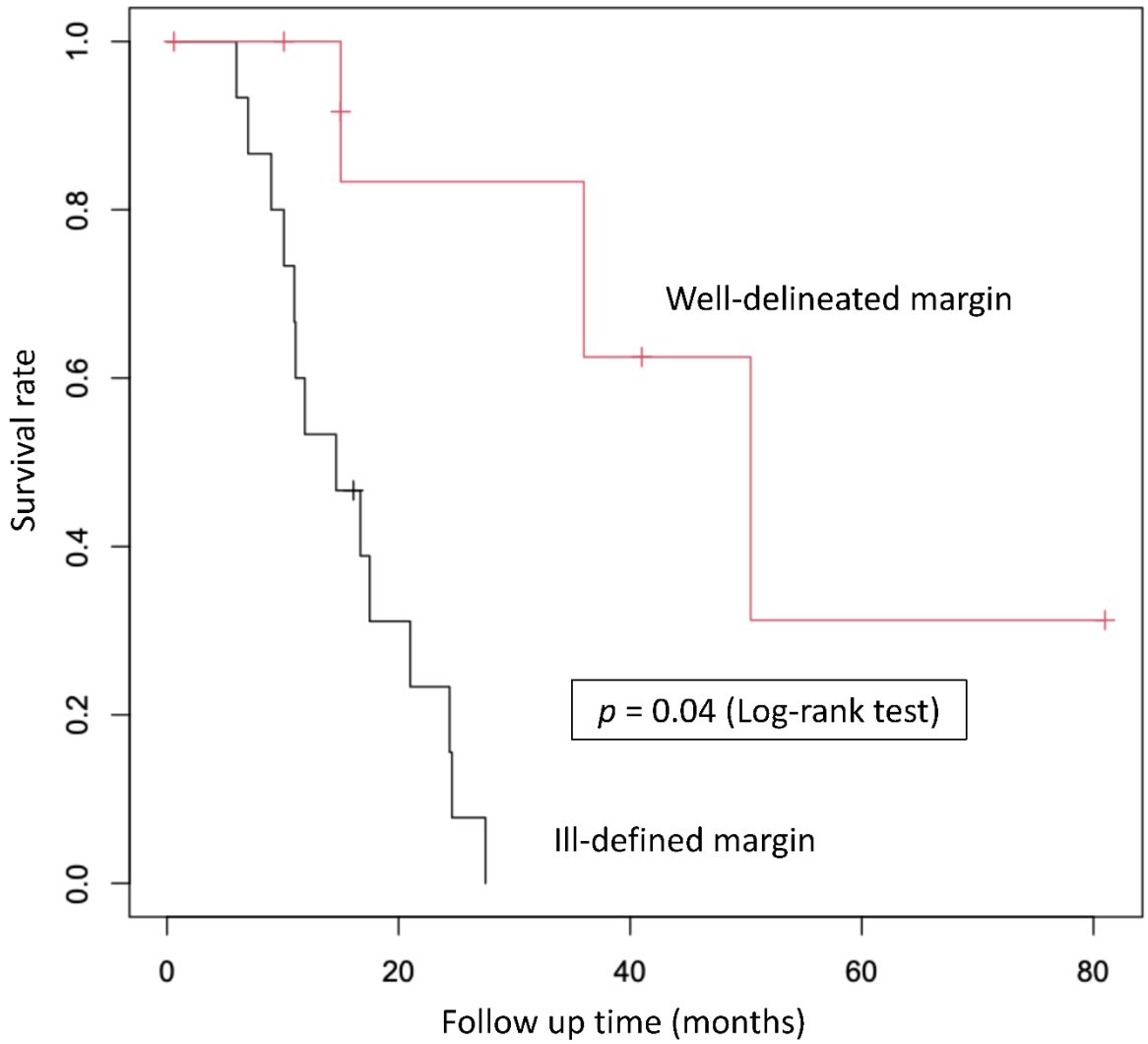

Figure 4. Kaplan–Meier curve with a log-rank test showed a significant difference in survival between patients with Diffuse hemispheric gliomas, H3 G34-mutant with an ill-defined margin (17 patients) and those with a well-delineated margin (30 patients; p = 0.04).